Chapter 4
Triboluminescence

Roman Nevshupa and Kenichi Hiratsuka

Abstract This works seeks to summarize recent advances in experimental studying of triboluminescence—defined here as the light emission when a material is subjected to rubbing, scratching, rolling, impacting or other mechanical agitation—and elucidate the basic mechanisms whereby triboluminescence is excited.

4.1 Introduction and Brief Historical Survey

Triboluminescence (TL) is defined by the Oxford English Dictionary as the emission of light from a substance caused by rubbing, scratching, or similar frictional contact [1] or, more generally, as the quality of emitting light at interacting surfaces in relative motion. It should be noted that the substance referred to in this definition may include both the materials of the contacting bodies and the surrounding gas or liquid, e.g., atmospheric air and lubricating oil.

The art of making fire by rubbing two wooden sticks together is a prehistoric example of how light emission can be produced by friction first due to incandescent radiation and then due to chemical reaction of wood oxidation [2]. Also triboluminescence can naturally occur when frictional contact is composed of dielectric materials susceptible of intensive frictional electrification. In this case triboluminescence is usually manifested by a shine or lightning around the frictional contact and is related to electrical discharge with gas or liquid. This phenomenon can be observed during precise turning of glassy polymers by a diamond tool in dry air [3], in which process weak glowing occurs around the cutting tool near the cutting edge as well as at the rake surface of the tool (see Fig. 4.1).

R. Nevshupa (✉)
IETCC, CSIC, C/Serrano Galvache 4, 28033 Madrid, Spain
e-mail: r.nevshupa@csic.es

K. Hiratsuka
Chiba Institute of Technology, 2-17-1 Tsudanuma,
Narashino-shi, Chiba 275-8588, Japan
e-mail: hiratsuka@sea.it-chiba.ac.jp

Fig. 4.1 *Side view* of the turning process of polycarbonate, showing light emission ($v_c = 1\,\text{m/s}$, $f = 5\,\mu\text{m/rev}$) (reprinted from [3] © 2004, with permission from CIRP)
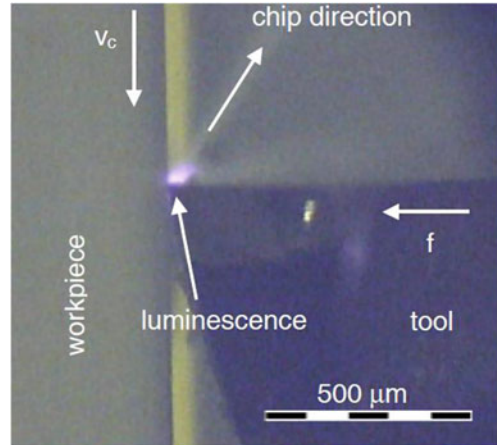
Luminous signals in the atmosphere such as glowing, light flashes and lightning, which result from fracture and slippage of rocks in earthquake-prone regions, are also attributed by many researchers to triboelectricity and triboluminescence [4–7]. These signals, which occur prior to, concurrently or after severe earthquakes, are a supreme manifestation of triboluminescence which can be observed on the Earth. Even more tremendous are the lightnings and sprites in volcanic plumes and dust devils in planets of our solar system and in the atmospheres of brown dwarfs and gas giant planets outside of our solar system [8]. Triboelectric charging of dust particles is frequently invoked as a mechanism for spectacular lightning discharges in dust clouds of silicate planetary regolith analogues [9].

Though the oldest records on systematic studies of triboluminescence comes from the beginning of the seventeenth century, the TL must surely be observed before [10]. Bearing in mind that the triboluminescence frequently accompanies triboelectrification, this phenomenon could probably be noticed since the remote antiquity, from the works on electrostatics of Thales of Miletus dated back to the sixth century BC. The knowledge on the triboluminescence developed in the period from the 17th century to the third quarter of the 20th century was reviewed from various perspectives by A. Walton. A comprehensive literature survey on mechanically induced luminescence for the period 1968–1998 can be found in [11].

The word *triboluminescence* was coined by Wiedeman in 1888 to denote the light emission resulting on fracturing materials [10]. In its long history *triboluminescence* was applied to various luminescent processes, some of which, at first sight, have little in common, e.g., emission during breaking of adhesive bonds [12, 13]; shaking of mercury in a glass vessel [14]; rapid crystallization of certain substances [15]; collapse of small gas bubbles in a liquid [16]; excitation of a laser-induced shock wave in solids [17]; elastic and plastic deformation of solids, scratching, milling and fracture [10, 18]. Though the forms of mechanical action significantly differ between these processes, many of them rely on quite similar physico-chemical reactions

(see Sect. 4.2). As a natural consequence of the diversity of the forms of mechanical action, in literature, the name *triboluminescence* is concurrently used as a synonym of *fractoluminescence*, *crystalloluminescence*, *sonoluminescence* and *piezolumines-cence,* all of which are different forms of *mechanoluminescence* [19]. In this work we endeavour to adhere to the original signification of *triboluminescence* as defined by the Oxford Dictionary, therefore, this chapter is focused principally on those tri-boluminescence phenomena which are directly related with tribological interaction between solids.

Even though the triboluminescence has been studied for centuries, this phenom-enon still remains something of an enigma at the conceptual and theoretical levels. Triboluminescence is intimately related to both friction and wear and all three require an understanding of highly nonequilibrium processes occurring at the molecular level [20]. These processes significantly differ depending on the tribological conditions, environment and materials. Furthermore, it is important to understand how all these elements come together producing synergetic coupling on different length and time scales.

Triboluminescence has great potential for the development of advanced materials, for example, the materials capable of sensing and imaging the stress intensity and distribution under applied load [21, 22]. The TL can be used, as well, for remote diagnosing of failures of space and vacuum mechanisms [23]. In medicine, the TL and triboemission from biological tissues have been applied for early diagnosing of cancer and other diseases [24, 25].

4.2 Basic Processes and Activation Mechanisms

During long time it was believed that frictional heating is the dominant mechanism for many tribophysical and tribochemical phenomena including triboluminescence. This belief was induced by the empirical evidence coming from the observation of heat generation in heavily loaded joints and brakes. Nevertheless, as early as 1792 Saussure demonstrated that in certain cases light could be obtained under such conditions that a pure temperature radiation was altogether unlikely [15].

The obvious contradiction related to the fact that frictional heating is weak or negligible under mild and light frictional conditions, and that the net temperature increase under these conditions is not sufficient to initiate TL was overcame by introducing the flash temperature [2] and magma–plasma concepts [26]. The main idea behind these concepts is that heat generation occurs on sub-micrometric zones of real contact, called hot spots, under almost adiabatic conditions. It was suggested that, while the total generated heat is quite low, the instant temperature increase on the minute hot spots can be sufficiently high to produce melting, thermionic electron emission, triboplasma and triboluminescence [27]. Though these hypothesis have been proven for high speed and relatively heavy-loaded contacts, there is still a lot of debates about the existence of hot spots and the extent of the temperature increase on them in lightly loaded and microscopic tribocontacts as well as under low sliding velocities [28].

In the studies of energy dissipation at sliding of various amorphous carbon coatings using molecular dynamic simulation it was found that the temperature increase on the hot spots was less than 300 °C even under severe sliding conditions: contact pressure in the range 7.6–56 GPa and sliding velocity 90.2 ms^{-1} [29, 30]. The temperature flashes were extremely short-time, in picosecond range, and subnanometer size. These findings corroborated that the mechanism which can confidently be ruled out is that the average mechanical energy fed in per atom of a material under such sliding conditions is sufficient to excite an atom directly into emitting visible or UV light [10, 15]. Different excitation mechanisms of triboluminescence must exist.

Various authors suggested that at a tribocontact mechanical energy is not converted instantaneously and fully into Joule heat. Though the major part of mechanical energy is converted into heat, there exist de-excitation pathways in which energy is transferred to different forms [31]. Deformation, bonds breaking and stress-induced chemical transformations resulting from quasi-adiabatic energy release excite various energy-rich states [18, 32–36], whereas subsequent de-excitation of these excited states promotes cascade of multiple emission processes. Radiation and radiationless de-excitation can lead to luminescence, emission of electrons and ions, chemical transformations, generation of electric and magnetic fields and so on. Collision of the emitted particles and photons with atoms and molecules can lead to the secondary excitation and decay processes and so on [37]. Thus, energy dissipation at the sliding contact is an extremely complex process involving a large variety of elementary physical processes and chemical reactions. These processes include incandescent radiation [36, 38], molecular deformation and direct mechanical excitation of electronic levels in mechanically affected zones [18, 36]; space charge generation due to cleavage, contact electrification [12, 36, 39, 40]; piezoelectric effect [21]; recombination of charged particles, holes and radicals [18, 21]; electric discharge through surrounding gas or liquid [10, 15, 39]; electroluminescence [10, 26]; photoluminescence [41]; cathode- and ionoluminescence [42]; resonance radiation from excited particles [10]; phase transformation [36]; gas adsorption and chemical reactions [26, 36]; unpinning and annihilation of dislocations, defect stripping, motion of charged dislocations [39]; and others.

In an exhaustive study involving 23 different materials and aimed at distinguishing the major possibilities for excitation of mechanoluminescence obtained by grinding the crystals in a glass tube, Sweeting [43] found two clearly distinct mechanisms of mechanoluminescence: (i) luminescence that requires a discharge through air or other surrounding gas and (ii) luminescence which comes from the processes within the crystal, possibly the release of energy from recombination of energetic defects. Some of the materials presented parallel action of both mechanisms. In addition, three separate modes were observed for the first excitation mechanism: excitation of the surrounding gas by electron bombardment; excitation of the photoluminescence of the material by electron bombardment; and excitation of the photoluminescence of the material by absorption of the ultraviolet (UV) emission of the excited gas.

Recently, rare-earth complexes have drawn the attention of many researchers since mechanoluminescence of these materials can be induced by mechanical deformation without fracture and without electric discharge. During deformation the strain

energy excites the filled traps to release holes to the valence band. The holes then excite rare-earth ions and return to the ground state by emitting light [44]. Another material that can repeatedly emit light without destruction is zinc sulphide doped with transition metal ions. Non-destructive mechanoluminescence materials are very promising candidates for the development of smart damage sensors capable of real-time detection of the magnitude and location of deformation within the material.

A number of experiments coupled to theoretical modelling have made great advances in unifying apparently diverse phenomena relative to mechanical activation of physical and chemical reactions and provided a crucial benchmark for mechanisms and behaviour of mechanoluminescence under elemental mechanical actions such as fracture, grinding or cohesive detachment [10, 15, 18, 21, 36, 40, 43]. Varentsov and Khrustalev [45] summarized these findings in a generalized scheme of the emission phenomena and chemical reactions occurring when solids are subjected to an external mechanical influence, mainly in form of deformation or fracture. This scheme is shown in Fig. 4.2 by black boxes and lines. The boxes highlighted in yellow designate various luminescence phenomena. This scheme was further developed by introducing other non-intuitive processes involved in the mechanical energy dissipation at frictional contact (blue boxes and lines). Excitation of metastable states just by contacting without deformation and fracture, e.g., due to contact electrification, is one of these processes. These new processes are specifically relative to frictional mechanical interaction and have not been considered within the framework of mechanoemission and mechanochemistry.

For tribo- and mechanoluminescence, a common basis underpins the behaviour on atomic and nanometer scale (Fig. 4.3b). However, as a natural consequence of a complex tribological behaviour characterized by synergism of processes and self-organization of structures across time and length-scales of several orders of magnitude, TL is a much more complex phenomenon than elementary mechanoluminescence. In the mechanoluminescence studies, in which the materials are usually milled, ground, strained or fractured, the geometry of interfaces is highly irregular, while the contact interactions and interface processes have a random character. In contrast, when the wear rate is low, the macroscopic geometry of tribological contacts in machines and in the nature is usually well-defined and stable or quasi-stable in time (see Fig. 4.3a). The overall geometry of a tribocontact keeps stable despite the fact that in each instant new surfaces come into contact [37]. Quasi-stable distribution of physical parameters (pressure, electric field, temperature, and so on) around a frictional contact associated to its temporal and geometric stability creates favourable conditions for spontaneous formation of complex, self-organized and thermodynamically steady dissipative structures, which can occur at significant distances from the real contact zone. This explains why the triboluminescence phenomena can span the length scales from the quantum to the astronomical one, while the mechanoluminescence related to fracture or milling usually does not occur beyond microscopic scale.
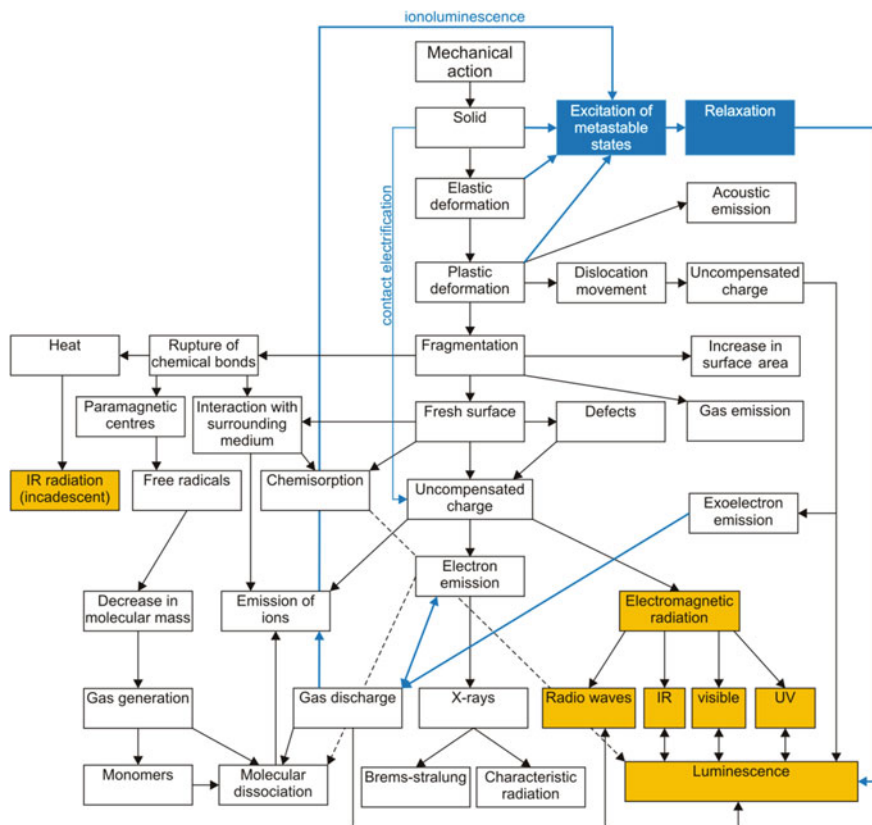
Fig. 4.2 Schematic drawing of some physical processes and chemical reactions involved in the mechanical energy dissipation at frictional contact and relevant triboemission and triboluminescence phenomena. *Black boxes* and *lines* correspond to the generalized scheme of the emission phenomena and chemical reactions occurring when solids are subjected to an external mechanical influence (reprinted from [45] © 1995, with permission from the Russian Academy of Sciences and Turpion Ltd). The *boxes* highlighted in *yellow* designate various luminescence phenomena. The *boxes* and *lines* highlighted in *blue* indicate the processes which are specifically related to frictional mechanical interaction and which have not been considered within the framework of mechanoemission and mechanochemistry

4.3 Experimental Techniques for Studying Triboluminescence

Triboluminescence occurs as a response of a system to the introduction of mechanical energy at a frictional contact. Thus, an experimental set-up for measuring the TL should necessarily have two main subsystems: (i) the tribological device for producing relative motion of two solids under controlled velocity and loading conditions and (ii) the optical system for measuring the intensity and spectral characteristics of the emitted light in different spectral ranges and on various time scales.
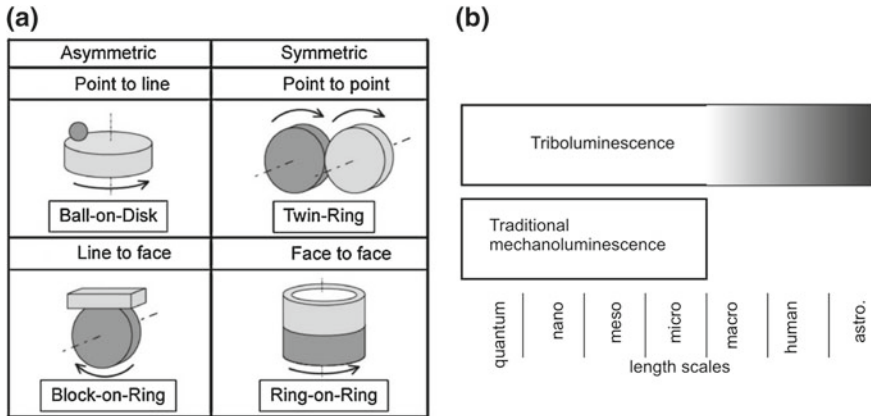
Fig. 4.3 a Classifications of contact configurations of four types of sliding-motion tribometers (reprinted from [46] © 2011, with permission from Elsevier). **b** Length scales of traditional mechanoluminescence and triboluminescence processes

Though in the past several experimental techniques for measuring the TL have been developed, only few of them can be considered as true tribological systems, i.e., the systems where two surfaces slide and/or roll past each other [39, 44, 47, 48], while most of other devices are aimed at grinding, milling, fracturing or straining the material being studied [18, 49, 50]. The reason for that relies on the misleading use of the term *triboluminescence* instead of *deformational luminescence* or *fracto-luminescence*.

Simultaneous scanning of both the friction force being a measure of the rate of mechanical energy dissipation and the TL is essential to reveal common mechanisms lying behind these processes. However, it is not an easy task because in the laboratory tests the TL occurs directly in the buried interface or in the close proximity to the contact zone, typically at the distance below 1 mm from it. If both solids being in frictional contact are non-transparent in the spectral range of interest for the TL study, the emitted photons can only be collected from the sides of the contact zone. In case one or both solids are transparent in this spectral range, the TL can be recorded either from the side or through the transparent solid.

The necessity to focus the optical system on a tiny luminescent zone buried in the interface rules out the tribometer configurations in which the contact zone is not stationary. This is why a pin-on-disk configuration with a stationary pin and rotating disk has been normally used in most of the TL studies. Schematic drawing of a typical experimental system with a pin-on-disk configuration aimed at the TL measurement through a transparent disk is shown in Fig. 4.4a. Light from the luminescent zone at the frictional contact passes through the quartz disk (Fig. 4.4b), a sapphire viewport and is condensed by lenses of an optical microscope. The light beam can be directed to a high-sensitive camera (in this case CCD) or to a spectrometer for the analysis of the spectral characteristics. Quartz and sapphire have been chosen because of the
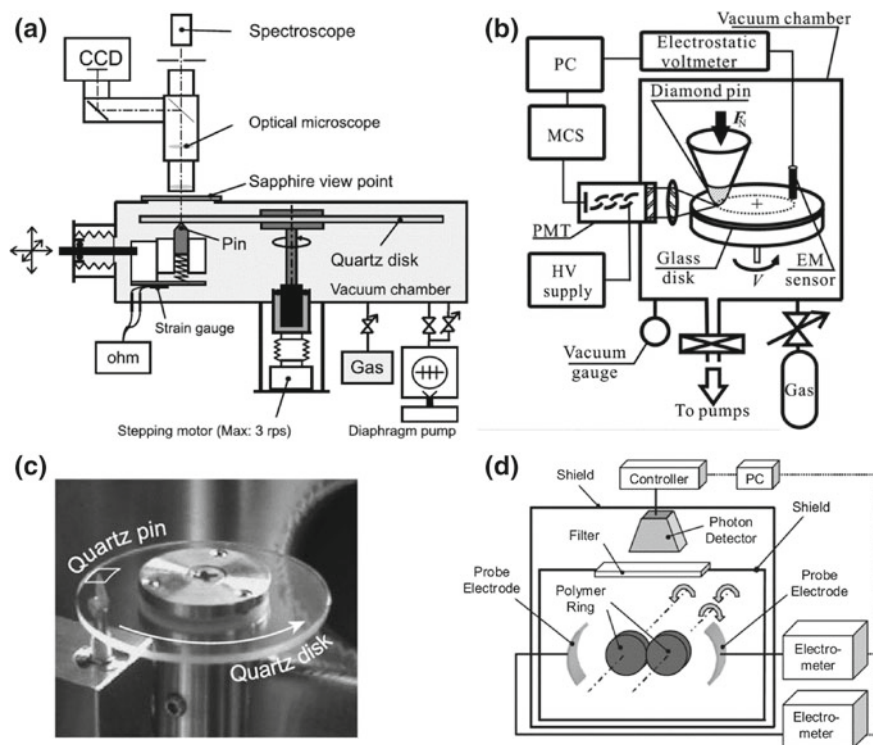
Fig. 4.4 **a** Schematic drawing of a pin-on-disk set-up in which spatial distributions and spectroscopic characteristics of the TL can be studied. Light passing through the quartz disk is measured from the opposite side of the contact by an optical microscope combined with a CCD camera and a spectrometer. **b** *Photograph* of the quartz pin and quartz disk. **c** Schematic drawing of the experimental vacuum tribometer with a pin-on-disk configuration in which the TL is measured from the side using a photomultiplier tube (PMT). Electric impulses at the anode of a PMT were acquired by a multichannel scaler (MCS). Surface potential was measured by an electrostatic voltmeter using an electromechanical (EM) sensor. **d** The twin-ring tribometer with a chemiluminescence analyzer. Photons passing through a filter are detected by a photomultiplier. Charges induced on the surfaces by rubbing are measured by an electrometer through an air probe electrodes which were set at the farthest end of the specimens without contacting them. (**a**) and (**b**) reprinted from [47] © 2006, with permission from Elsevier; (**c**) reprinted from [51] © 2003, with permission from American Institute of Physics; (**d**) reprinted from [52] © 2012, with permission from Elsevier

transmission in the ultraviolet (UV) and visible (vis) ranges. The disk and the pin are placed inside a vacuum chamber, so both the gas pressure and the composition can be controlled. By introducing specific optical filters in the optical path of the microscope the TL can be studied in different spectral ranges.

Another example of a TL pin-on-disk system in which the emitted photons are measured from the side is shown in Fig. 4.4c. In this system light is condensed by a lens which is used also as a viewport of a vacuum chamber and guided to a photomultiplier tube (PMT). The output signal of the PMT is acquired by a multichannel

scaler (MCS). The PMT can operate in either current mode or pulse count mode. In the pulse count mode, nanosecond resolution of the TL signal can be achieved.

The disadvantages of the pin-on-disk configuration are related to asymmetric sliding conditions: different wear rate of the disk and the pin, extremely large difference in the area of the contact zone on the pin and on the disk, dissimilar adsorption conditions and so on [52]. These shortcomings have been removed in the twin-ring tribometer (Fig. 4.4d) [46]. In addition to the sliding motion this tribometer allows to do pure rolling or rolling/sliding with controlled slip ratio. Due to symmetrical configuration the surface charge can be measured on both surfaces and simultaneously with the TL.

4.4 Characteristics of the TL

4.4.1 Spatial Distribution of the TL at a Tribological Contact

K. Nakayama and his research group were probably the first who succeeded to measure two-dimensional spatial distribution of the TL at a sliding contact. They used a pin-on-disk tribometer situated in the ambient air [39, 53, 54] or in a vacuum chamber [54–56] and intensified CCD camera equipped with CaF_2 lenses transparent in UV, vis and IR ranges.

Figure 4.5a shows the unfiltered pseudo-colour image of in plane spatial intensity distribution of the TL taken through the disk. The images represent integrated TL intensity in approx. 12 disk revolutions. TL completely surrounded the contact zone and spread out to the distances up to $200\,\mu m$ from the centre of the contact in the direction of the relative disk motion (shown by the arrow). The total TL was the most intensive in the zone situated behind the contact at a distance of approx. $50\,\mu m$ from its centre. Figure 4.5b shows the intensity distribution of the TL intensity in UV range. For the total TL and UV TL the shape of the intensity distributions were
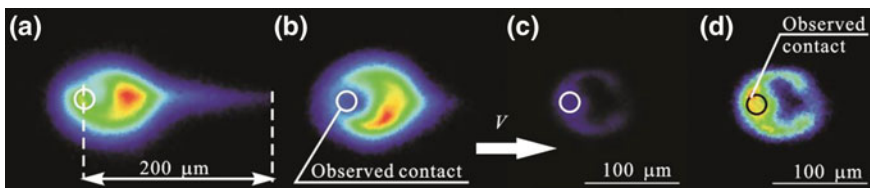

Fig. 4.5 Two-dimensional spatial distribution of the TL at the sliding contact of a diamond pin (radius of curvature $300\,\mu m$) and a sapphire disk in ambient air. **a** unfiltered pseudo-colour *image*; **b** band-filtered pseudo-colour *image* of the TL in the range 290–420 nm; **c** band-filtered pseudo-colour *image* of the TL in the range 720–2800 nm; **d** enhanced *image* from (**c**). A *circle* in each *figure* denotes the size and position of the nominal contact area determined visually using optical microscopy (reprinted from [54] © 2003, with permission from ASME)

quite similar, although small variation in shape can be ascribed to the fluctuations of the TL in time [39] since the images in Fig. 4.5 were acquired sequentially. The total luminescent power was also quite similar in both cases. That was taken as indicating that the TL arose mainly from the excitation of nitrogen from the surrounding air. Spectroscopic measurements generally corroborated this hypothesis (see Sect. 4.4.2).

The TL intensity in IR range was low (Fig. 4.5c) and exhibited unexpected distribution. Figure 4.5d presents the enhanced image of the IR TL from Fig. 4.5c. Apart from IR radiation at the contact area that can be ascribed to the frictional heating there were two lateral branches aside from the friction track protruding from the contact zone in the direction of disk rotation. The shape of the IR TL intensity distribution was defined as an open circle or a horseshoe. The most surprising was the fact that IR luminescence on the zones of the branches was much more intense than on the friction track behind the contact although these branch zones had not been in contact with the pin. These findings suggested that the gas discharge at a friction contact can be an important channel of energy dissipation and a source of the surface/gas heating inside and outside the friction track.

Miura et al. [53] found that the TL can also occur in front of the sliding contact. This luminescent zone, designated γ in Fig. 4.6, situated at a distance from the centre of the contact almost twice larger than the luminescent zone β behind the contact. Nitrogen excitation in electrical gas discharge was identified as the main mechanisms of the TL in the zones β and γ since most of the light was emitted in the UV range. Other regular and irregular patterns of the TL intensity distribution were described by various authors, e.g., four strong emission points connected each other and surrounding a dark zone just behind the contact to form a ring, elongated tails, irregular strips aside the friction track which spanned for more than hundred micrometres behind the contact and so on [55, 57, 58]. The characteristics of some of these TL features and the reasons of their occurrence are discussed in the following sections.

The size and the shape of the luminescent zone strongly depended upon the surrounding gas pressure. Figure 4.7 shows a series of pseudo-colour images of the TL under various pressures of dry air [55]. While the gas pressure decreased from the
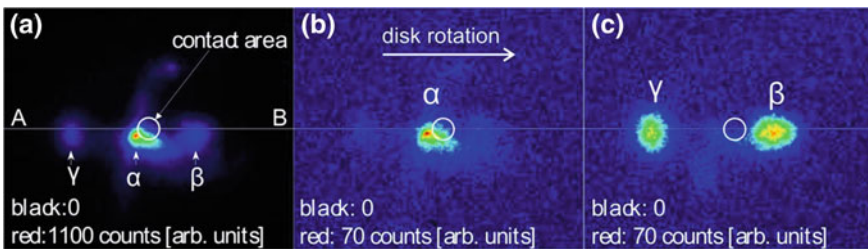

Fig. 4.6 **a** unfiltered pseudo-colour *image* of the TL during sliding in air; **b** band-filtered pseudo-colour *image* of the TL in the range 610–780 nm; **c** band-filtered pseudo-colour *image* of the TL in the range 300–420 nm. The size of all images is $250 \times 300\,\mu m^2$. *Red colour* corresponds to the maximum intensity indicated in each *figure*. A *circle* shows the position and the size of the contact area (reprinted from [53] © 2001, with permission from American Institute of Physics)
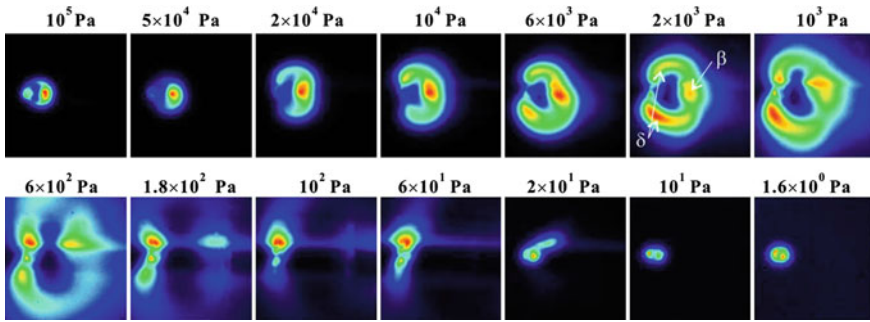
Fig. 4.7 Unfiltered pseudo-colour images of the TL obtained during sliding of a diamond pin on a sapphire disk under various pressures of dry air (reprinted from [55] © 2004, with permission from Elsevier)

atmospheric to 600 Pa the size of the luminescent zone expanded more than six-fold. It deserves special attention the fact that when the gas pressure decreased below 10 kPa the zone of the maximum TL intensity shifted from the position behind the contact (β) to lateral positions aside the contact zone designated hereinafter δ. When the gas pressure further decreased below 600 Pa the TL zone rapidly shrank. The luminescent zones β, γ and δ disappeared below 20 Pa, whereas weak light emission could be observed solely at the contact zone (zone α in Fig. 4.6). Though the expansion of the luminescent zone with the decreasing gas pressure followed by its collapse resembles typical behaviour of gas discharge, e.g., glowing discharge in a tube [59] or corona [60], the behaviour of the TL is much more complex because of the complex geometry and the configuration of the electric field.

4.4.2 Effect of the Ambient Gas and the Material of the Counterbodies on Spectral Characteristics and Intensity Distribution of the TL

When the TL of insulating materials occurs in air, important part of light emission comes from lightning as indicated by the characteristics lines of N_2 discharge in the TL spectrum [54, 57, 61]. Nakayama and Nevshupa [54] studied the TL spectra for diamond pin—sapphire disk configuration in various gas and compared the obtained TL spectra with the glowing discharge spectra of the same gases. They found that the TL emission spectra in air, N_2, O_2, He and CH_4 were very similar to the spectra of the glowing discharge, although the proportion between various peaks was slightly different (compare, for example, Figs. 4.8a and b, 4.9a and d). In H_2 the glowing discharge spectrum had one strong line $H_\alpha = 656.279$ nm, which, however, was not found in the TL emission spectrum. In ethane and propane neither the TL nor the glowing discharge spectra had any noticeable feature.

Fig. 4.8 a The TL spectrum
for diamond-sapphire sliding
in He atmosphere. **b** The
luminescence emission
spectrum of glowing
discharge in He (reprinted
from [54] © 2003, with
permission from ASME)
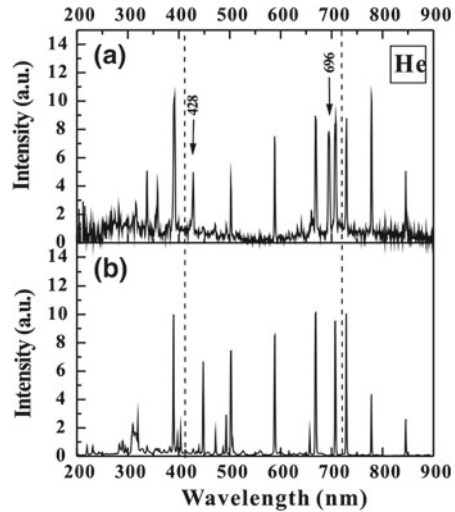
Apart from the emission corresponding to the gas discharge a line at approximately
696 nm was observed in all TL spectra with exception for ethane and propane, but
not in the glowing discharge spectra of the same gases (Figs. 4.8 and 4.9a). This line
was only found when sapphire disk was used in the test (Fig. 4.9a–c). In accurate
study Nakayama [57] confidently demonstrated that this line should be attributed to
the ^{2}E metastable state luminescence of Cr impurities in sapphire (694.5 nm). Also
he showed that the irregular stripes on the sides of the friction track in the images
of the TL spatial distribution corresponded to this luminescence component. These
stripes began at the lateral branches of the TL and spanned more than 100 μm behind
the contact zone [55, 57]. While the intensity of the gas discharge luminescence
stabilized after 2–3 min, the intensity of the induced luminescence from sapphire
slowly increased in time and reached a steady value after 7 min that corresponded
to approximately 1,100 disk revolutions [54]. Though the excitation mechanism for
the secondary luminescence from sapphire is not clear yet, both the gas discharge
luminescence and mechanical activation should be ruled out since the luminescence
occurred outside the friction track and the origin of the luminescent zones did not
coincide with the zone of the maximal discharge luminescence. This luminescence
can probably be excited by electron [43, 57] or ion [42, 62] bombardment.

The ease of gas discharge increases as the pressure decreases, but it decreased
again when the density becomes too low and the mean free path of electrons becomes
too large for sustaining the discharge. In high vacuum the gas discharge is sup-
pressed and the light emission occurred mainly from the contact zone. This explains
the observed behaviour of the spatial distribution of the TL (Fig. 4.7). Miura et al.
[62] studied spectral characteristics of light emitted from the contact zone in high
vacuum for different pin materials. For diamond pin and quartz disk configura-
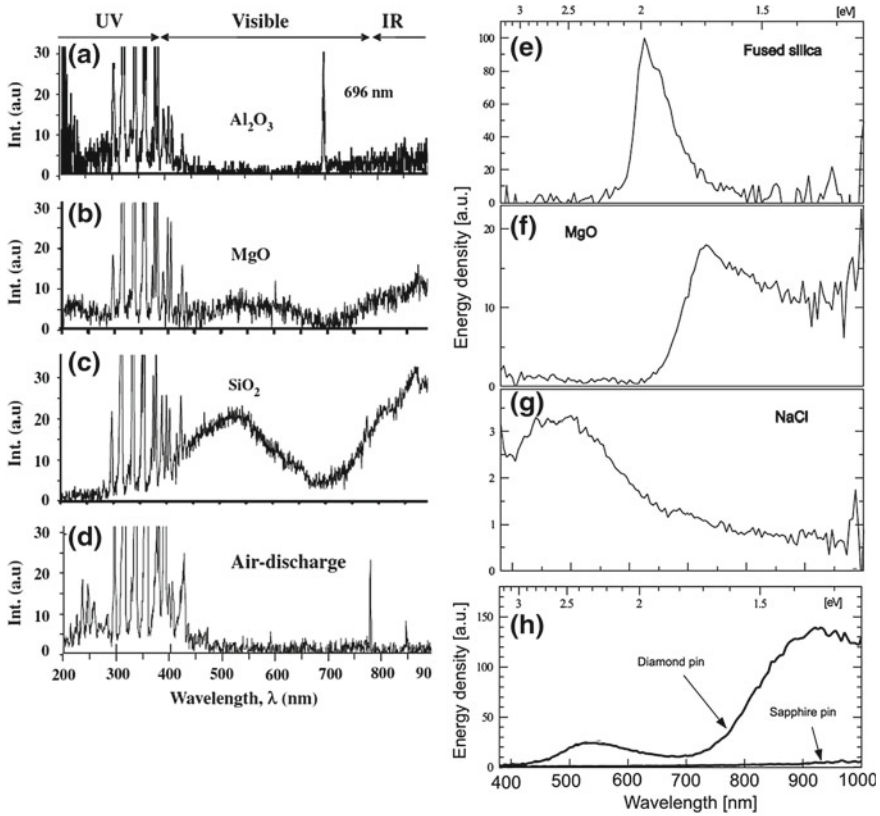tion they observed three broad bands at 400, 630 and 900 nm. The measured bands

Fig. 4.9 Effect of material of the disk (**a**)–(**c**) and the pin (**e**)–(**h**) on the spectral characteristics of the TL. **a** A natural diamond pin and a synthetic sapphire disk; **b** a natural diamond pin and a MgO disk; **c** a natural diamond pin and a crystal SiO$_2$ disk; **d** spectrum of the luminescence of glowing discharge in air; **e** a synthetic fused silica pin and a synthetic sapphire disk; **f** a MgO single crystal pin and a synthetic sapphire disk; **g** a NaCl pin and a synthetic sapphire disk; **h** a natural diamond pin and a synthetic sapphire disk. **a**–**c** measured in ambient air; **e**–**h** measured in vacuum (10^{-3} Pa). (**a**)–(**d**) reprinted from [57] © 2010, with permission from Springer Science and Business Media. (**e**)–(**h**) reprinted from [62] © 2009, with permission from Elsevier

significantly differed from the theoretical Planck's distribution and did not depend on the sliding conditions. These findings led the authors to the conclusion that thermal radiation was not the dominant mechanism of the luminescence excitation. The band at 900 nm (Fig. 4.9h) was caused by fractoluminescence of diamond. In addition to the broad band at 900 nm another weak band between 350 and 650 nm was observed during diamond abrasion (Fig. 4.9h). For the ionic crystals studied in [62] the TL emission spectra were very similar to the corresponding fractoluminescence spectra and were related to electronic excitation of vacancies or impurities during abrasion. For quartz, the band at 630 nm (Fig. 4.9e) was ascribed to fractoluminescence of non-bridging oxygen hole centres. Broad band in the TL emission spectrum of MgO

(Fig. 4.9f) was attributed to the emission of Mn and Cr^{3+} impurities and was similar to thermoluminescence and photoluminescence spectra of MgO.

4.4.3 Effect of Friction Type and Humidity on the TL and Triboelectrification of Polymers

Despite a number of works on triboluminescence of ceramics, only limited researches have been carried out in the field of polymers. Nowadays, polymers are used for numerous machine parts and the TL phenomena can have undesired effect on their operation life, safety and reliability. As polymers can be easily charged during friction, triboluminescence is likely to occur wherever polymers are in rubbing contact. However, not much attention has been paid on the TL of polymers since the TL usually occurs in the UV range, while if the TL is visible, its effect is often neglected. The gas discharge associated with the TL from polymers releases charged particles and photons of extremely high specific energy.

The mechanism of Triboelectrification (TE) is essential for the process of the TL. However, it is difficult to measure how much charge has been generated. This is because the measured charge on each surface reflects the resultant charge after the recombination of charges as a result of the discharge between them as well as charge leakage through the bulk or on the surface. However, charge can be measured when the gas discharge is suppressed and the materials of high electrical resistance are used. The twin-ring tribometer (Figs. 4.3a and 4.4d) is the most appropriate for this purpose, because it enables the sequential measurements of both the TE and the TL. Additionally, this test rig has the advantage of realizing the rolling and sliding contacts by just reversing the rotation direction of one specimen. The following results are obtained from this apparatus.

Figure 4.10 compares the charging processes of polyamide (PA66) and polytetrafluoroethylene (PTFE) in sliding and rolling contacts together with the associated photon emission. Sliding or rolling occurred in the period between 25 and 75 s of the data records. During sliding the TL intensity was two orders of magnitude higher than during rolling, whereas the saturation charge in both experiments was almost the same. It should be mentioned that during the first revolution of the cylinders in the sliding test the discharge did not occur, therefore the measured surface charge reached the maximum. In rolling friction, the surface charges gradually increased with time. These clearly indicated that the charge accumulation rate during sliding was higher than during rolling. This fact can be attributed to the multiple real contacting of the same surface zones during sliding. The decrease in the TL intensity during sliding which is seen in Fig. 4.10a can be related to the gradual transfer of PTFE onto PA66, which would transform the rubbing pair from PA66/PTFE to PTFE/PTFE. Therefore, the charging rate per contact/separation on similar material decreased leading to the corresponding decrease in the TL intensity.
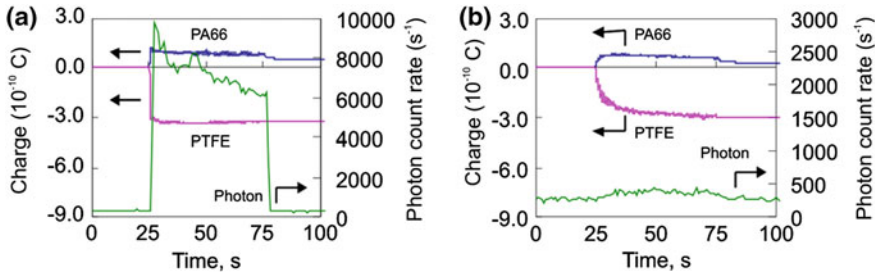
Fig. 4.10 TE and TL processes during sliding (**a**) and rolling (**b**) between PA66 and PTFE. (reprinted from [52] © 2012, with permission from Elsevier)

The fact that the TL from the sliding contact of polymers reached its maximum soon after the onset of rubbing indicated that the luminescence could not be attributed to the frictional heating. Rather, photon emission was triggered by the electron emission which could be caused by the following two mechanisms: fracto-emission and field emission. In contrast to rolling friction, sliding friction produces continuous fracture of the material in the contact zone. Therefore, electrons can be emitted from the fractured surface. Frictional electrification contributes to the build-up of a strong electric field which can induce field electron emission.

Environmental humidity is one of the most influential factors in triboelectrification [63], which would then give rise to the change in TL. Figure 4.11 shows a typical result of the effect of humidity on the TE and TL from the rubbing between acrylonitrile butadiene styrene (ABS) and PTFE. When relative humidity (RH) increased from 0 to 58 % the TL intensity also increased. This process was associated with the increase in the surface charge that was especially intensive between 10 and 58 %. However, the saturation charge on both polymers at 10 % RH was higher than at both 0 and 58 %. The relationship between the charging rate/saturation charge and photon amount led to the conclusion that TL rate is determined by the charging rate per one frictional contact and not by the saturation charge on the surface. It is worth mentioning that almost no TL could be observed at 0 % RH, although the leakage rate is expected to be the lowest. This finding can be due to the limited number of charge carrier which
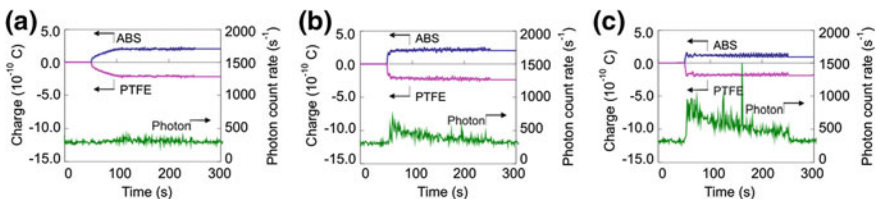

Fig. 4.11 Effects of humidity on the triboelectrification and triboluminescence in the rubbing between ABS and PTFE at various relative humidity: **a** 0 %, **b** 10 % and **c** 58 % (reprinted from [52] © 2012, with permission from Elsevier)
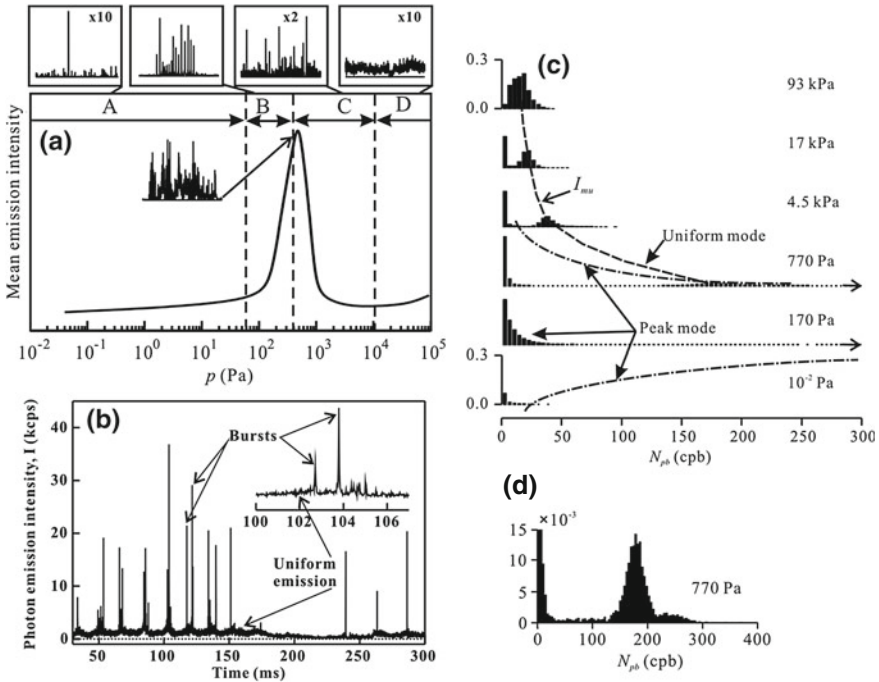
Fig. 4.12 **a** The effect of the Ar pressure on the total TL intensity and behaviour patterns (reprinted from [42] © 2013, with permission from IOP Publishing Ltd); **b** fragment of the TL time series measured with a resolution of 20.48 μs (reprinted from [51] © 2003, with permission from American Institute of Physics); **c** histograms of the TL time series distributions on intensity at various pressures of Ar atmosphere; **d** a histogram of the TL time series distributions at gas pressure 770 Pa showing two components: the *bell-shape* and the exponential-like

inhibits a subsequent discharge between surfaces. This means that charges have to be carried by ions (H_3O^+ and OH^-) generated from the adsorbed water [64]. On the other hand, when the relative humidity increased to a certain value, the surface charge decreased due to discharge and recombination.

4.4.4 Behaviour of the TL on Different Time Scales

Gas pressure is an important external parameter not only for the intensity and spatial distribution of the TL related to the gas discharge, but also for its behaviour on various time scales [42, 51]. In the experiments with a diamond pin—sapphire disk configuration four behaviour patterns of the TL time series depending on the Ar gas pressure were distinguished (Fig. 4.12a) [42]: at $p < 20$ Pa the TL was of low intensity with sparse irregular bursts. In the range 20 Pa $< p < 300$ Pa the TL had a regular pattern consisting of a series of groups of almost equally spaced bursts (Fig. 4.12b).

The period between the bursts varied from 20 to 40 ms, whereas the groups of the bursts appeared synchronously with the disk rotation. In the range $300\,\text{Pa} < p < 10\,\text{kPa}$, uniform emission with irregular bursts occurred. At the pressure higher than 10 kPa only weak uniform emission was observed. The appearance of burst with the frequency of 33 Hz is puzzling since the typical frequencies of the gas discharge oscillation is three to four orders of magnitude higher.

Density distribution functions of the PMT output time series on the number of photon counts per time bin are shown in Fig. 4.12c. The distributions have either exponential-like or the bell-shaped distributions, or the combination of both (see, for example, Fig. 4.11d). The exponential-like distribution component was ascribed to the burst TL mode, while the bell-shaped one was attributed to the uniform mode. From the analysis of the density distribution function it was found that the uniform mode increased in intensity when the gas pressure decreased from 100 kPa to 300 Pa and vanished below 300 Pa. The burst mode also increased with decreasing gas pressure and reached maximum at 170 Pa. Then it decreased, but not totally vanished.

4.5 Modelling Approach

Electric gas discharge being an important excitation mechanism for the TL still remains poorly understood. From the point of view of electrostatics, pin-on-disc configuration can be considered as an extreme case of a point-to-plane gap with a point being in contact with a plane. In the case of insulating electrodes the gas discharge, referred to as barrier or silent discharge, is likely to be a very complex process because of the displacement field and very low mobility of charges in the electrodes [65]. Furthermore, in contrast to traditional barrier discharge being driven by alternating feeding potential, the polarities of the pin and the disk are rather stable [42, 51].

When embarking on a study of electric gas discharge at a sliding contact the first question which should be addressed is related to the configuration and the strength of electric field. Bearing in mind the constrain geometry and possible alteration of the electric field by introducing conductive measuring electrodes, direct measuring of the electric field in a gap around the contact zone is not a trivial task. The electric field can be roughly estimated if the rate of the charge generation is known. The latter was determined from the surface potential on the disk measured in high vacuum when the gas discharge is hindered (Fig. 4.13a) [66]. For the sliding contact composed of a diamond pin (r 1000 µm) and a sapphire disk under the normal load 0.96 N and sliding velocity 4.4 cm s^{-1} (1 rps) the rate of the charge generation was 3.39×10^{-11} A. Then, taking into account the geometry of the friction zones on the pin and the disk and assuming that, in this rough and ready approach, the charge leakage through the solid and on the surfaces can be neglected, the configuration of the electric field was modelled using finite elements method (Fig. 4.13b).

The negative charge on the disk had no effect on the radial component of the electric field, which was dominant, and only minor effect on the axial component. It was concluded that concentrated positive charge on the pin controlled the overall
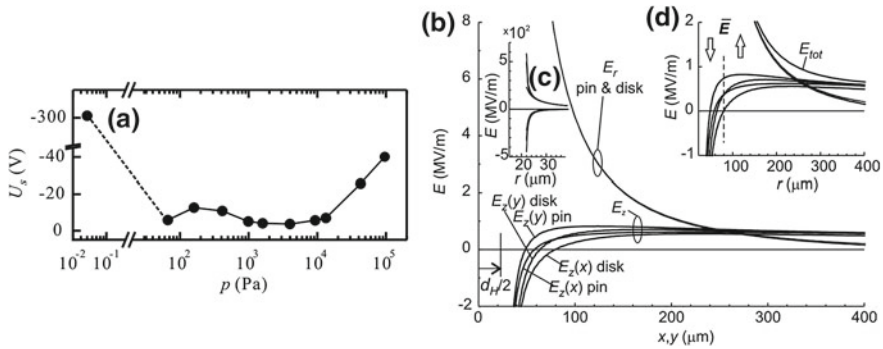
Fig. 4.13 a Mean electrostatic potential measured 2 mm above the friction zone on the disk as function of gas pressure. **b** Radial, E_r, and axial, $E_x(x)$ and $E_y(y)$, components of the electric field along the *x*- and *y-axes* on the disk and pin surfaces near the contact zone. *Insets* **c** and **d** show the *graphs* on different scales (reprinted from [66] © 2013, with permission from IOP Publishing Ltd)

configuration of the electric field. This can explain the experimental finding that the gas discharge occurred even from the disk which had a 5 nm thick conductive Al coating [67]. The electric field was highly non-uniform that contrasted with the common believe and other models based on the assumption of near symmetric bipolar configuration of the electric field in the gap [57, 68]. Such configuration of the electric field with a highly stressed anode and a low-field cathode is typical for positive corona discharges.

The strong and negative axial component of the electric field near the contact zone provided necessary conditions for the emission of triggering electrons through a field emission mechanism. An analysis of impact ionization and secondary processes at various gas pressures [42] showed that the corona model provided plausible explanations for the experimentally observed TL behaviour (Sect. 4.4.4) consisting of various combinations of two main modes. It was shown that when the region of electron collision ionization coincides with both the regions of the secondary processes and triggering electron emission, the TL emission is uniform. At lower pressures the first two regions decouple leading to the instability of the gas discharge and appearance of bursts.

References

1. "Triboluminescence", *Oxford Dictionaries*. (Oxford University Press, Oxford, 2010)
2. H. Blok, The flash temperature concept. Wear **6**, 483–94 (1963)
3. G.P.H. Gubbels, G.J.F.T. van der Beek, A.L. Hoep, F.L.M. Delbressine, H. van Halewijn, Diamond tool wear when cutting amorphous polymers. CIRP Annal. Manuf. Technol. **53**, 447–450 (2004)
4. F. Freund, Charge generation and propagation in igneous rocks. J. Geodyn. **33**, 543–570 (2002)
5. F. St-Laurent, J.S. Derr, F.T. Freund, Earthquake lights and the stress-activation of positive hole charge carriers in rocks. Phys. Chem. Earth Parts A/B/C **31**, 305–312 (2006)
6. T.V. Losseva, I.V. Nemchinov, Earthquake lights and rupture processes. Nat. Hazards Earth Syst. Sci. **5**, 649–656 (2005)
7. J. Muto, H. Nagahama, T. Miura, I. Arakawa, Frictional discharge at fault asperities: origin of fractal seismo-electromagnetic radiation. Tectonophysics **431**, 113–122 (2007)
8. C. Helling, M. Jardine, D. Diver, S. Witte, Dust cloud lightning in extraterrestrial atmospheres. Planet. Space Sci. **77**, 152–157 (2013)
9. A.A. Sickafoose, J.E. Colwell, M. Horányi, S. Robertson, Experimental investigations on photoelectric and triboelectric charging of dust. J. Geophys. Res. Space Phys. **106**, 8343–8356 (2001)
10. A.J. Walton, Triboluminescence. Adv. Phys. **26**, 887–948 (1977)
11. L.J. Kricka, J. Stroebel, P.E. Stanley, Triboluminescence: 1968–1998. Luminescence **14**, 215–220 (1999)
12. B.V. Derjaguin, N.A. Krotova, Y.P. Toporov, in *Emission of High-Speed Electrons and Other Phenomena Accompanying the Process of Breaking Adhesion Bonds*, ed. by J.M. Georges. Tribology Series (Elsevier, Amsterdam, 1981), pp. 471–87
13. T. Miura, M. Chini, R. Bennewitz, Forces, charges, and light emission during the rupture of adhesive contacts. J. Appl. Phys. **102**, 103509–103516 (2007)
14. Experience faite a l'observatoire sur le barometre simple touchant un nouveau phenomene qu'on ya découvert. Le Journal des sçavans (Académie des inscriptions et belles-lettres, Paris, France, 1676)
15. H.B. Weiser, I.I. Crystalloluminescence, J. Phys. Chem. **22**, 576–595 (1917)
16. M.P. Brenner, S. Hilgenfeldt, D. Lohse, Single-bubble sonoluminescence. Rev. Mod. Phys. **74**, 425–484 (2002)
17. Y. Tsuboi, T. Seto, N. Kitamura, Laser-induced shock wave can spark triboluminescence of amorphous sugars. J. Phys. Chem. A **112**, 6517–6521 (2008)
18. P.Y. Butyagin, The luminescence accompanying mechanical deformation and rupture of polymers. Vysokomol soyed **A12**, 290–299 (1970)
19. B.P. Chandra, K.K. Shrivastava, Dependence of mechanoluminescence in rochelle-salt crystals on the charge-produced during their fracture. J. Phys. Chem. Solids **39**, 939–940 (1978)
20. M. Urbakh, J. Klafter, D. Gourdon, J. Israelachvili, The nonlinear nature of friction. Nature **430**, 525–528 (2004)
21. B.P. Chandra, Mechanoluminescence of nanoparticles. Open Nanosci. J. **5**, 45–58 (2011)
22. J.-C. Zhang, C.-N. Xu, S. Kamimura, Y. Terasawa, H. Yamada, X. Wang, An intense elastico-mechanoluminescence material $CaZnOS:Mn^{2+}$ for sensing and imaging multiple mechanical stresses. Opt Express **21**, 12976–12986 (2013)
23. E.A. Deulin, V.P. Mikhailov, Y.V. Panfilov, R.A. Nevshupa, *Mechanics and Physics of Precise Vacuum Mechanisms* (Springer, Dordrecht, 2010)
24. V.E. Orel, I.N. Kadyuk, N.N. Dzyatkovskaya, M.I. Danko, Y.I. Mel'nic, Mechanoluminescence: lymphocyte analysis after exposure to ionizing radiation. Luminescence **15**, 29–36 (2000)
25. V.E. Orel, A.V. Romanov, N.N. Dzyatkovskaya, I. Mel'nik, The device and algorithm for estimation of the mechanoemisson chaos in blood of patients with gastric cancer. Med. Eng. Phys. **24**, 365–371 (2002)

26. G. Heinike, *Tribochemistry* (Carl Hanser Verlag, Munchen, 1984)
27. B. Vick, M.J. Furey, An investigation into the influence of frictionally generated surface temperatures on thermionic emission. Wear **254**, 1155–1161 (2003)
28. R. Nevshupa, The role of athermal mechanisms in the activation of tribodesorption and triboluminisence in miniature and lightly loaded friction units. J. Frict. Wear **30**, 118–126 (2009)
29. J.D. Schall, G. Gao, J.A. Harrison, Effects of adhesion and transfer film formation on the tribology of self-mated DLC contacts. J. Phys. Chem. C **114**, 5321–5330 (2010)
30. T.-B. Ma, Y.-Z. Hu, H. Wang, Molecular dynamics simulation of shear-induced graphitization of amorphous carbon films. Carbon **47**, 1953–1957 (2009)
31. A.I. Rusanov, Thermal effects in mechanochemistry. Russ. J. Gen. Chem. **72**, 327–344 (2002)
32. P.Y. Butyagin, Problems in mechanochemistry and prospects for its development. Russ. Chem. Rev. **63**, 965 (1994)
33. P.Y. Butyagin, Structural disorder and mechanochemical reactions in solids. Russ. Chem. Rev. **53**, 1025–1038 (1984)
34. T.E. Fischer, Tribochemistry. Annual review material. Science **18**, 303–323 (1988)
35. S.L. Craig, Mechanochemistry: a tour of force. Nature **487**, 176–177 (2012)
36. B.P. Chandra, S. Tiwari, M. Ramrakhiani, M.H. Ansari, Mechanoluminescence in centrosymmetric crystals. Cryst. Res. Technol. **26**, 767–781 (1991)
37. R.A. Nevshupa, Triboemission: an attempt of generalized classification, in *Tribology: Science Applications*, ed. by C. Kajdas (PAS, Vienna, 2004), pp. 11–25
38. J. Thevenet, M. Siroux, B. Desmet, Measurements of brake disc surface temperature and emissivity by two-color pyrometry. Appl. Therm. Eng. **30**, 753–759 (2010)
39. K. Nakayama, R.A. Nevshupa, Plasma generation in a gap around a sliding contact. J. Phys. D Appl. Phys. **35**, L53–L56 (2002)
40. V.A. Kluev, T.N. Vladikina, Y.P. Toporov, V.J. Anisimova, B.V. Derjaguin, Emission phenomena accompanying the triboelectrification process in vacuum. IEEE Trans. Ind. Appl. **IA-14**, 544–546 (1978)
41. J.P. Duignan, I.D.H. Oswald, I.C. Sage, L.M. Sweeting, K. Tanaka, T. Ishihara et al., Do triboluminescence spectra really show a spectral shift relative to photoluminescence spectra? J. Lumin. **97**, 115–126 (2002)
42. R.A. Nevshupa, Effect of gas pressure on the triboluminescence and contact electrification under mutual sliding of insulating materials. J. Phys. D Appl. Phys. **46**, 185501 (2013)
43. L.M. Sweeting, Triboluminescence with and without Air. Chem. Mater. **13**, 854–870 (2001)
44. C.N. Xu, Coatings, in *Encyclopedia of Smart Materials*, ed. by M. Schwartz (Willey, New York, 2002), pp. 190–201
45. E.A. Varentsov, Y.A. Khrustalev, Mechanoemission and mechanochemistry of molecular organic crystals. Russ. Chem. Rev. **64**, 783–797 (1995)
46. K. Hiratsuka, T. Yoshida, The twin-ring tribometer–characterizing sliding wear of metals excluding the effect of contact configurations. Wear **270**, 742–750 (2011)
47. J. Muto, H. Nagahama, T. Miura, I. Arakawa, Frictional discharge plasma from natural semiconductor/insulator junctions: origin of seismo-electromagnetic radiation. Phys. Chem. Earth Parts A/B/C **31**, 346–351 (2006)
48. K. Nakayama, H. Hashimoto, Effect of surrounding gas pressure on Triboemission of charged particles and photons from wearing ceramic surfaces. Tribol. Trans. **38**, 35–42 (1995)
49. G.E. Hardy, J.I. Zink, Triboluminescence and pressure dependence of the photoluminescence of tetrahedral manganese(II) complexes. Inorg. Chem. **15**, 3061–3065 (1976)
50. L.M. Sweeting, J.L. Guido, An improved method for determining triboluminescence spectra. J. Lumin. **33**, 167–173 (1985)
51. R.A. Nevshupa, K. Nakayama, Triboemission behavior of photons at dielectric/dielectric sliding: time dependence nature at 10^{-4}-10^4 s. J. Appl. Phys. **93**, 9321–9328 (2003)
52. K. Hiratsuka, K. Hosotani, Effects of friction type and humidity on triboelectrification and triboluminescence among eight kinds of polymers. Tribol. Int. **55**, 87–99 (2012)
53. T. Miura, K. Nakayama, Two-dimensional spatial distribution of electric-discharge plasma around a frictional interface between dielectric surfaces. Appl. Phys. Lett. **78**, 2979–2981 (2001)

54. K. Nakayama, R.A. Nevshupa, Characteristics and pattern of plasma generated at sliding contact. J. Tribol-T Asme **125**, 780–787 (2003)
55. K. Nakayama, R.A. Nevshupa, Effect of dry air pressure on characteristics and patterns of tribomicroplasma. Vacuum **74**, 11–17 (2004)
56. K. Nakayama, The plasma generated and photons emitted in an oil-lubricated sliding contact. J. Phys. D Appl. Phys. **40**, 1103–1107 (2007)
57. K. Nakayama, Triboplasma generation and triboluminescence: influence of stationary sliding partner. Tribol. Lett. **37**, 215–228 (2010)
58. K. Nakayama, Mechanism of triboplasma generation in oil. Tribol. Lett. **41**, 345–351 (2011)
59. Y.P. Raizer, *Gas Discharge Physics* (Springer, New York, 1991)
60. L.B. Loeb, *Electrical Coronas, Their Basic Physical Mechanisms* (University of California Press, Berkley, 1965)
61. T. Miura, K. Nakayama, Spectral analysis of photons emitted during scratching of an insulator surface by a diamond in air. J. Appl. Phys. **88**, 5444–5447 (2000)
62. T. Miura, E. Hosobuchi, I. Arakawa, Spectroscopic studies of triboluminescence from a sliding contact between diamond, SiO_2, MgO, NaCl, and Al_2O_3 (0001). Vacuum **84**, 573–577 (2009)
63. E. Németh, V. Albrecht, G. Schubert, F. Simon, Polymer tribo-electric charging: dependence on thermodynamic surface properties and relative humidity. J. Electrost. **58**, 3–16 (2003)
64. L.S. McCarty, G.M. Whitesides, Electrostatic charging due to separation of ions at interfaces: contact electrification of ionic electrets. Angewandte Chemie Int. Ed. **47**, 2188–2207 (2008)
65. H.E. Wagner, R. Brandenburg, K.V. Kozlov, A. Sonnenfeld, P. Michel, J.F. Behnke, The barrier discharge: basic properties and applications to surface treatment. Vacuum **71**, 417–436 (2003)
66. R. Nevshupa, Effect of gas pressure on the triboluminescence and contact electrification under mutual sliding of insulating materials. J. Phys. D Appl. Phys. **46**, 185501 (2013)
67. R.A. Nevshupa, K. Nakayama, Effect of nanometer thin metal film on triboemission of negatively charged particles from dielectric solids. Vacuum **67**, 485–490 (2002)
68. K. Nakayama, M. Tanaka, Simulation analysis of triboplasma generation using the particle-in-cell/Monte Carlo collision (PIC/MCC) method. J. Phys. D Appl. Phys. **45**, 495203 (2012)